

Transient crosslinking controls the condensate formation pathway within chromatin networksZong-Pei Wu,¹ Kerry S. Bloom², M. Gregory Forest³ and Xue-Zheng Cao^{1,*}¹*Department of Physics at Xiamen University, Xiamen 361005, P.R. China*²*Department of Biology, University of North Carolina at Chapel Hill, Chapel Hill, North Carolina 27599, United States*³*Departments of Mathematics, Applied Physical Sciences and Biomedical Engineering, University of North Carolina at Chapel Hill, Chapel Hill, North Carolina 27599, United States*

(Received 10 September 2023; accepted 26 February 2024; published 5 April 2024)

The network structure of densely packed chromatin within the nucleus of eukaryotic cells acts in concert with nonequilibrium processes. Using statistical physics simulations, we explore the control provided by transient crosslinking of the chromatin network by structural-maintenance-of-chromosome (SMC) proteins over (i) the physical properties of the chromatin network and (ii) condensate formation of embedded molecular species. We find that the density and lifetime of transient SMC crosslinks regulate structural relaxation modes and tune the sol-vs-gel state of the chromatin network, which imparts control over the kinetic pathway to condensate formation. Specifically, lower density, shorter-lived crosslinks induce sollike networks and a droplet-fusion pathway, whereas higher density, longer-lived crosslinks induce gellike networks and an Ostwald-ripening pathway.

DOI: [10.1103/PhysRevE.109.L042401](https://doi.org/10.1103/PhysRevE.109.L042401)

Nucleolus or nucleolar organizer regions (NORs), the key membraneless organelle governing the biological functions of eukaryotic cells, is composed of the genes for ribosomal RNA (rDNA), nascent ribosomal RNA transcripts (rRNA), and ribosomal proteins [1–10]. The nucleolus is able to expand in size, as well as modulate the number and size of nucleolar clusters during the fusion or ripening process, which reflects the cellular demand for ribosomes [11–15]. Individual genes in the nucleus, including rDNA, can reposition in response to environmental cues [16–19]. The ripening process of nucleoli and the equilibrium structure of clustered nucleoli are sensitively dependent on nonequilibrium biological processes, like RNA transcription, that can modulate the crosslinking topology of the chromatin network [20–25]. The chromatin network contained in undifferentiated cell nuclei, with a large transcriptional potential, is known to be dynamic, similarly for the chromatin network found adjacent to the nuclear envelope [26–28]. Heat shock or heavy metal stress also has the effect of spurring a densely packed chromatin network within the nucleus to be more dynamic [29–31].

The assembly principles responsible for the ripening mechanism of nuclear bodies and nucleoli have been widely investigated experimentally and theoretically [32–42]. It is now well established that chromatin polymers within the nucleus are dynamically activated via transient, noncovalent interactions by structural-maintenance-of-chromosome (SMC) proteins, e.g., condensins and cohesins [43–48]. An emerging challenge is to reveal mechanistic details of the coarsening process and pathways to condensate formation of nuclear bodies in general, and in particular, how these fundamental cellular processes are controlled by transient SMC

crosslinking of the chromatin network that regulate relevant cellular functions.

The focus in this Letter is the ability of transient SMC crosslinking kinetics to tune the viscoelastic environment of the chromatin network, and thereby regulate the pathway to condensate formation of molecular species embedded within [49–52]. In the molecular dynamics (MD) simulations, chromatin is modeled as a coarse-grained bead-spring polymer chain. The ensemble of chromatin chains is activated by SMC proteins that induce transient bead-bead crosslinks between nonnearest neighbor beads [53–55]. We idealize a chromatin network with $N_c = 100$ polymer chains, each consisting of $l_c = 128$ beads. For this study, we impose that one in four beads within each chain, uniformly spaced, is “active,” i.e., capable of forming a condensin crosslink with another active chromatin bead either within or between chains. For each fixed set of crosslink kinetic parameters, we compute two outcome statistics: the mean crosslink lifetime, τ_{life} , and the mean crosslink density, c_{xlink} . In the model, we embed $N_{\text{sm}} = 1280$ small-molecule beads (SMBs), each the size of one chromatin bead, where each SMB is endowed with a short-range Lennard-Jones attraction to all other SMBs that allows aggregation and condensate formation of the embedded SMBs, see the Supplemental Material [56].

The simulated development of condensate formation of embedded SMBs is shown in the upper right and lower panels of Fig. 1(a) for short-lived and 1(b) for long-lived SMC-chromatin crosslinks. As the coarsening process evolves, number growths of individual droplets indicate that SMBs embedded in both the short- and long-lived crosslinked networks continue to aggregate to an eventual single droplet. However, ripening in the long-lived crosslinked network is slower than in the short-lived crosslinked network, although the networks have identical c_{xlink} . More specifically, over the timescale range $810 \text{ s} < t < 1890 \text{ s}$ in each system, two

*xzcao@xmu.edu.cn

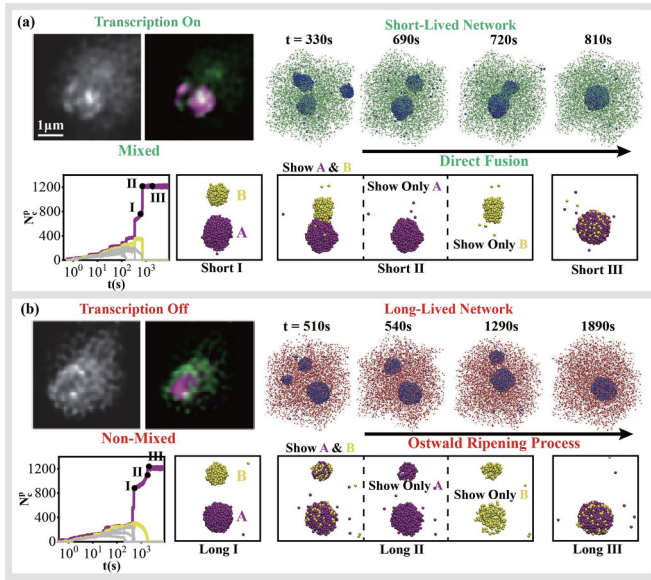


FIG. 1. Coarsening and condensation of small molecular species embedded within crosslinked chromatin networks. Top left corner panels (a) and (b) are experimental images (Copyright ©2021, Oxford University Press) showing transcription-tuned structure of the nucleolus by displaying two separated components in green and purple, and their mixtures in white [24]. Simulation snapshots show coarsening and condensate formation processes of embedded SMB complexes in the short-lived [top right panel (a)] vs long-lived [bottom right panel (b)] crosslinked networks. Here, $c_{\text{link}} = 11 \mu\text{m}^{-3}$ for both networks, and $\tau_{\text{life}} = 17\tau_0 = 0.51\text{s}$ for the short-lived network while the exaggerated limit of infinite lifetime is set for the long-lived one. The plots given in the lower and left panels (a) and (b) show the time-dependent evolution of the number of embedded SMBs contained in individual droplets, with the purple and yellow curves representing the SMB growth within the two largest droplets. Snapshots of the corresponding two largest SMB droplets during the processes of direct fusion in the short-lived network (labeled as Short I, Short II, and Short III) and Ostwald ripening in the long-lived network (labeled as Long I, Long II, and Long III) are displayed by the snapshots shown in the lower and right parts of each panel.

phase-separated SMB droplets remain within the long-lived crosslinked network, whereas the process has already coarsened to a single droplet within the short-lived crosslinked network. The development of experimental nucleolar condensates within chromatin chains, with transcription on and off corresponding to the simulation models of short-lived and long-lived crosslinked networks, are presented as snapshots in the upper left panels of Figs. 1(a) and 1(b), respectively [24]. In the experiments, different nuclear components are mixed or unmixed when the transcription is on or off, which match the simulations of showing two phase-separated nonchromatin droplets or a single droplet within the long-lived or short-lived crosslinked network over a large time range.

The coarsening of SMBs in the short- and long-lived crosslinked networks are qualitatively different, as shown by the lower panels of Figs. 1(a) and 1(b). In the long-lived crosslinked network, individual SMBs exchange between the two droplets during coarsening. As the system evolves, a positive net number of SMBs switch from the smaller to larger

droplet, and this directional flux gradient results in growth of the larger droplet at the expense of the smaller droplet. By associating this coarsening process with Ostwald ripening [57], the time-dependent evolution of distribution field $c(\vec{r}, t)$, of SMBs, outside the two droplets is assumed to be satisfied with the diffusion equation

$$\frac{\partial c(\vec{r}, t)}{\partial t} = D\nabla^2 c(\vec{r}, t), \quad (1)$$

where D defines the diffusion coefficient of individual SMBs. The local concentrations of SMBs at the boundaries of the droplets are given by the Gibbs-Thomson relation [58]:

$$c(r = R_1, t) = c_\infty \left(1 + \frac{2\gamma v}{k_B T R_1} \right),$$

$$c(r = \Delta R_c, t) = c_\infty \left(1 + \frac{2\gamma v}{k_B T R_2} \right), \quad (2)$$

where c_∞ , γ , and v give the dilute concentration threshold, the surface tension of droplets, and the volume of single SMB, respectively. The mass center separation between the two droplets, and the radii of the large and small droplets are denoted as ΔR_c , R_1 , and R_2 , respectively. At any given time, the net influx of SMBs joining the large droplet is given by [57]

$$J = \frac{8\pi\gamma c_\infty v D}{k_B T} \frac{\frac{R_1}{R_2} - 1}{1 - \frac{R_1}{\Delta R_c}}. \quad (3)$$

Due to influx of SMBs resulting in increasing continuously the volume of the large droplet, there is

$$dV_1/dt = vJ. \quad (4)$$

On the other hand, the volume of the large droplet is proportional to the number N_1 of SMBs contained in it,

$$V \approx N_1 \frac{4}{3}\pi \left(\frac{\sigma}{2} \right)^3, \quad (5)$$

in which $N_1 \approx N_{\text{sm}} - N_2$, with N_{sm} and N_2 being the number of SMBs contained in the whole system and in the small droplet, respectively. By combing the above equations, we obtain a theoretical expression for the dynamic growth of the larger droplet

$$\frac{dN_1(t)}{dt} = C * \frac{N_1^{1/3}(t)}{[N_{\text{sm}} - N_1(t)]^{1/3}} - 1, \quad (6)$$

with $C = \frac{48\gamma c_\infty v^2 D}{k_B T}$. Figure 2 presents a comparison of the theoretical formula and simulation results, which supports the Ostwald ripening pathway to condensates. In contrast, during the coarsening process of SMBs embedded in the short-lived crosslinked chromatin network, aggregation of droplets arises through their direct fusion.

We now associate the above differences in embedded SMB coarsening and condensate formation with the timescale- and lengthscale-dependent structural relaxation of the SMC-crosslinked chromatin network. Early in the coarsening process, the SMB droplet size, $D_{\text{drop}}(t)$, is less than the mean contour length of chain strands between crosslinks, l_{cross} , giving a rough estimate of the mean pore size distribution of the

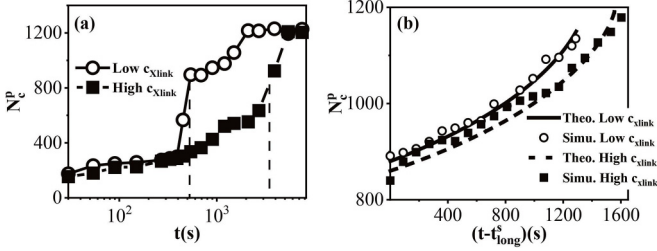


FIG. 2. (a) Temporal evolution of the number of embedded SMBs contained in the largest droplet within long-lived crosslinked chromatin networks at $c_{\text{xlink}} = 11 \mu\text{m}^{-3}$ and $25 \mu\text{m}^{-3}$. The vertical dashed lines show the corresponding threshold timescales, t_{long}^s , above which Ostwald ripening begins. (b) The observed simulation data and the corresponding theoretical fits based on Eq. (1) for dynamic growth of the largest droplets. The threshold timescales are $t_{\text{long}}^s = 600$ s and 1200 s for the simulations with $c_{\text{xlink}} = 11 \mu\text{m}^{-3}$ and $25 \mu\text{m}^{-3}$, respectively.

crosslinked network. However, as $D_{\text{drop}}(t)$ grows to and above l_{cross} , the fluctuations, or lack thereof in l_{cross} , become steering agents in the pathway of SMB droplet coarsening. In the long-lived SMC-crosslinked chromatin network, the pore size distribution is crystallized, hindering droplet fusion while allowing flux of single SMBs or small SMB complexes between droplets, thereby favoring the Ostwald ripening mechanism for coarsening and condensation. However, in the short-lived crosslinked network, the local pore sizes and pore size distribution fluctuate, releasing the rigid barrier to fusion of nearby droplets, thereby favoring coarsening by droplet fusion, a faster pathway to condensation.

The existence of “open channels for droplet fusion” in the short-lived crosslinked network is further supported from an energy perspective. We quantify the Jarzynski potential of mean force (PMF) between two distinct but nearby droplets with $R_{\text{drop}} > l_{\text{cross}}$ [59–61],

$$\Delta F(\Delta R_C) = -\frac{1}{\beta} \ln(\exp[-\beta W(\Delta R_C)]), \quad (7)$$

where $\beta = 1/k_B T$, and ΔR_C is the mass center distance between the separated droplets. The PMF between two droplets as shown in Fig. 3 is obtained by running MD simulations to mimic quasistatic processes, starting from an initial state represented by the Long I or Short I in Fig. 3. $W(\Delta R_C)$ is the work required to overcome the resistance induced by the merger of relaxed vs unrelaxed chromatin chains during a quasistatic process when the droplet mass center distance is ΔR_C . The PMFs plotted versus ΔR_C indicate that two droplets in the short-lived crosslinked network can fuse without external forces as a result of structural relaxation of the network on scales exceeding the droplet sizes. In contrast, there is a significant energy barrier to direct fusion of droplets in a long-lived crosslinked network because of an unrelaxed crosslink topology on lengthscales encompassing the droplet sizes.

Next, we seek to more deeply understand the network relaxation-droplet growth balance across the spatial and temporal scales that we surmise is controlling the mode of droplet-scale diffusion within a chromatin network, and thereby the condensate pathway selection of droplet fusion

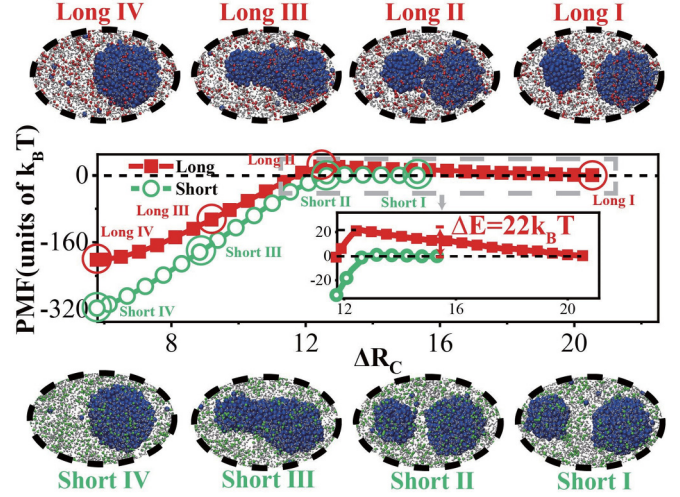


FIG. 3. The potentials of mean force (PMF) between the two largest SMB droplets in the short- and long-lived networks are plotted in green and red curves in the middle panel, respectively. Here, the settings of c_{xlink} and τ_{life} for the short- and long-lived networks are the same as those set in the Fig. 1. In the plots, ΔR_C defines the distance between the centers of mass of the two clusters. The corresponding structural evolution of the two droplets in the short- and long-lived networks is shown in the upper and lower panels, respectively.

vs Ostwald ripening. We begin with a Rouse-mode analysis of the relaxation spectra of the crosslinked chromatin chains over all length scales ranging from one monomer to the full chain length N . For the p th Rouse mode $X_p(t)$,

$$X_p(t) = \left(\frac{2}{N}\right)^{1/2} \sum_{i=1}^N r_i \cos\left[\frac{p\pi}{N}\left(i - \frac{1}{2}\right)\right], \quad (8)$$

the corresponding averaged autocorrelation function, $\langle X_p(t) \cdot X_p(0) \rangle$, describes the dynamic relaxation of a subchain containing N/p monomers (beads), where p is an integer between one and $N = 128$. Results in Fig. 4(b) reveal (i) chromatin chains in a sufficiently short-lived, low-density, crosslinked network can relax all Rouse modes, whereas, (ii) for chromatin chains in a sufficiently long-lived, densely crosslinked network, structural relaxation is prohibited for all chromatin subchains on lengthscales longer than l_{cross} . Based on fitting $\langle X_p(t) \cdot X_p(0) \rangle$ to a stretched exponential function [62],

$$\langle X_p(t) \cdot X_p(0) \rangle = \langle X_p^2 \rangle \exp[-(t/\tau_p)^{\beta_p}], \quad (9)$$

with β_p the stretching exponent, we obtain the critical timescale, τ_p , for chromatin subchains containing N/p monomers to complete their structural relaxation.

The growth timescale of droplets within short- and long-lived crosslinked networks are shown in Fig. 4(a), in which τ_{drop}^D denotes the timescale above which the third-largest droplet vanishes and $D_{2\text{nd}}$ defines the diameter of the second-largest SMB droplet at this timescale. We find $\tau_{\text{drop}}^D = 540$ s and $\tau_{\text{drop}}^D = 720$ s for the second-largest droplet to grow to a diameter of $D_{2\text{nd}} = 1.1 \mu\text{m}$ in the short- and long-lived crosslinked networks, respectively. On the chain relaxation

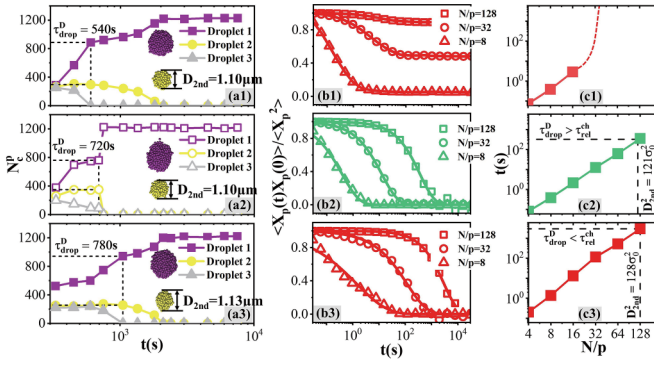


FIG. 4. Network relaxation-droplet growth balance. (a) Time-dependent evolution of the number of embedded SMBs contained in the three largest droplets during coarsening by case (I) Ostwald ripening in the long-lived network with $c_{\text{link}} = 11 \mu\text{m}^{-3}$ and $\tau_{\text{life}} = +\infty$; case (II) droplet fusion in the short-lived network with $c_{\text{link}} = 11 \mu\text{m}^{-3}$ and $\tau_{\text{life}} = 0.51\text{s}$; and case (III) Ostwald ripening in the short-lived network with $c_{\text{link}} = 22 \mu\text{m}^{-3}$ and $\tau_{\text{life}} = 5.1\text{s}$. (b) Time-dependent autocorrelation functions of selected Rouse modes of chromatin chains within the three networks considered in cases (I)–(III). (c) Relaxation timescales of chromatin subchains versus contour lengths for the three networks considered in cases (I)–(III). The red dash curve plotted in (c1) is to indicate that, for the long-lived network, the relaxation timescales of chromatin subchains converge to infinity when $\frac{N}{p}$ is larger than the contour lengths (with mean l_{cross}) of chain strands between crosslinks.

side of the network relaxation-droplet growth balance, a polymer subchain with random coiled diameter of $D_{\text{coil}}^{\text{ch}} = 1.1 \mu\text{m}$ contains up to $(D_{\text{coil}}^{\text{ch}})^2/\sigma_0 = 121$ monomers. As shown in Fig. 4(c), a subchain strand of $N/p = 121$ beads in the short-lived crosslinked network completes its structural relaxation on a timescale $\tau_{\text{rel}}^{\text{ch}}(N/p = 121)$ shorter than $\tau_{\text{drop}}^{\text{D}}(D_{2\text{nd}}/\sigma_0 = 11)$. This indicates that chromatin chains surrounding the second-largest droplet are sufficiently relaxed to open a “channel” larger than the droplet, allowing it to take a droplet-scale diffusion to merge with the largest droplet. To the contrary, chromatin chains in the long-lived crosslinked network do not relax on lengthscales at or above the contour length of subchains between neighboring crosslinks, presenting a barrier to diffusive merging of droplets of that size. However, smaller network scales are relaxed in the long-lived crosslinked network, allowing SMB subcomplexes within the smaller droplet to be pulled by the strong cumulative attractive force of the larger SMB droplet, draining complexes from the smaller to the larger droplet, i.e., coarsening via Ostwald ripening.

Modulating c_{link} and τ_{life} , as represented by the change from case (II) to case (III) in Fig. 4(a), delays the structural relaxation of the chromatin chains across all lengthscales [Fig. 4(b)], resulting in the relaxation of the crosslinked chromatin network to be slower than the growth of the phase-separated SMB droplets within the network. This scenario hinders diffusion at the droplet scale, thereby preventing droplet fusion and favoring Ostwald ripening. By systematically quantifying the network relaxation-droplet growth balance, the phase diagram in Fig. 5 shows the pathway to condensate formation, either droplet fusion (green) or Ostwald ripening (red), versus c_{link} and τ_{life} . Corresponding to,

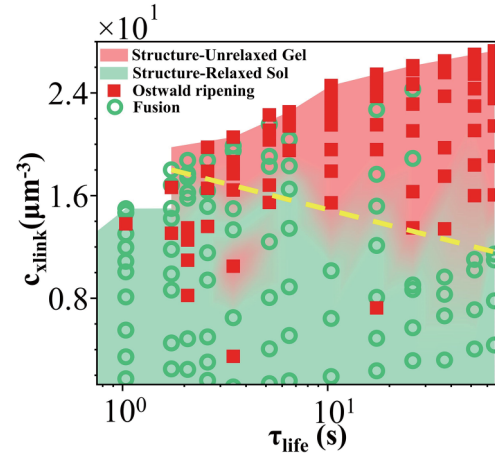


FIG. 5. Phase diagram of the condensate pathway of embedded SMBs within the chromatin crosslinked network versus τ_{life} and c_{link} . The colored background that labels the viscoelasticity of the chromatin network was superimposed after quantifying the network relaxation-droplet growth balance as done in Fig. 4. The dashed yellow line depicts the soft, stochastic boundary between the red and green regions.

respectively, a case that the crosslinked chromatin network is or is not sufficiently relaxed to open a “channel” large enough for droplet-scale diffusion, the crosslinked chromatin network is shown in Fig. 5 to be a structure-relaxed sol or structure-unrelaxed gel when $\tau_{\text{drop}}^{\text{D}} < \tau_{\text{rel}}^{\text{ch}}$ or $\tau_{\text{drop}}^{\text{D}} > \tau_{\text{rel}}^{\text{ch}}$ on the lengthscale of $N/p = (D_{2\text{nd}})^2$. As indicated in the phase diagram, the condensation pathway, direct fusion versus Ostwald ripening, is selected by the structure-relaxed sol versus structure-unrelaxed gel viscoelasticity of the crosslinked chromatin network.

In summary, we employ statistical physics modeling, superimposed with SMC-protein crosslinking kinetics, to show how SMC crosslinks manage the network relaxation-droplet growth balance between length and time scales that select the pathway to molecular condensate formation within the chromatin network. Lower (higher) c_{link} and τ_{life} induce a sollike (gellike) chromatin network, faster (slower) droplet and condensate formation, and a droplet fusion (Ostwald ripening) condensation pathway of embedded molecular species. The ability of SMC-activated chromatin networks to select pathways and rates of condensate growth is a striking illustration of genetic control of biological processes within the nucleus. The dynamic aggregation of small molecular species embedded within chromatin networks, that is difficult to quantify experimentally across all protein-to-organelle spatial and temporal scales, dictates how cells establish membraneless organelles essential for diverse cellular functions. The present study provides a computational and theoretical physics basis for understanding how cells acquire specificity in making distinctions to pull from different clusters of small molecular species embedded within diverse viscoelastic cellular environments.

The research of Z.P.W. and X.Z.C. was supported in part by the National Science Foundation of China through Grant NSFC-11974291 and the Natural Science Foundation of Fujian Province of China (No. 2020J01009). The research of

M.G.F. was partially supported by the U.S. National Science Foundation Award No. CISE-1931516 and the Alfred E. Sloan

Foundation Award No. G-2021-14197. The research of K.S.B. was partially supported by the NIH-R01-GM32238.

- [1] L. Montanaro, D. Treré, and M. Derenzini, *Am. J. Pathol.* **173**, 301 (2008).
- [2] S. F. Banani, H. O. Lee, A. A. Hyman, and M. K. Rosen, *Nat. Rev. Mol. Cell Biol.* **18**, 285 (2017).
- [3] J. R. Buchan, *RNA Biol.* **11**, 1019 (2014).
- [4] M. Feric, N. Vaidya, T. S. Harmon, D. M. Mitrea, L. Zhu, T. M. Richardson, R. W. Kriwacki, R. V. Pappu, and C. P. Brangwynne, *Cell* **165**, 1686 (2016).
- [5] F. Frottin, F. Schueder, S. Tiwary, R. Gupta, R. Körner, T. Schlichthaerle, J. Cox, R. Jungmann, F. U. Hartl, and M. S. Hipp, *Science* **365**, 342 (2019).
- [6] F. Ritossa and S. Spiegelman, *Proc. Natl. Acad. Sci. USA* **53**, 737 (1965).
- [7] G. J. Sullivan, J. M. Bridger, A. P. Cuthbert, R. F. Newbold, W. A. Bickmore, and B. McStay, *EMBO J.* **20**, 2867 (2001).
- [8] S. Boeynaems, S. Alberti, N. L. Fawzi, T. Mittag, M. Polymenidou, F. Rousseau, J. Schymkowitz, J. Shorter, B. Wolozin, L. Van Den Bosch *et al.*, *Trends Cell Biol.* **28**, 420 (2018).
- [9] D. L. J. Lafontaine, J. A. Riback, R. Bascetin, and C. P. Brangwynne, *Nat. Rev. Mol. Cell Biol.* **22**, 165 (2021).
- [10] C. Martin, S. Chen, A. Maya-Mendoza, J. Lovric, P. F. G. Sims, and D. A. Jackson, *J. Cell. Sci.* **122**, 1551 (2009).
- [11] S. F. Banani, A. M. Rice, W. B. Peeples, Y. Lin, S. Jain, R. Parker, and M. K. Rosen, *Cell* **166**, 651 (2016).
- [12] P. S. Amenta, *Anat. Rec.* **139**, 155 (1961).
- [13] J. Kim, K. Y. Han, N. Khanna, T. Ha, and A. S. Belmont, *J. Cell. Sci.* **132**, jcs.226563 (2019).
- [14] C. P. Brangwynne, T. J. Mitchison, and A. A. Hyman, *Proc. Natl. Acad. Sci. USA* **108**, 4334 (2011).
- [15] V. Rajshekar, O. Adame-Arana, G. Bajpai, S. Safran, and G. H. Karpen, *Biophys. J.* **123**, 39a (2024).
- [16] Y. He, J. Lawrimore, D. Cook, E. E. Van Gorder, S. C. De Larimat, D. Adalsteinsson, M. G. Forest, and K. Bloom, *Nucleic Acids Res.* **48**, 11284 (2020).
- [17] J. Dekker and T. Misteli, *Cold Spring Harb Perspect. Biol.* **7**, a019356 (2015).
- [18] M. van Sluis and B. McStay, *Genes Dev.* **29**, 1151 (2015).
- [19] J. A. Villegas, M. Heidenreich, and E. D. Levy, *Nat. Chem. Biol.* **18**, 1319 (2022).
- [20] J. Berry, S. C. Weber, N. Vaidya, M. Haataja, and C. P. Brangwynne, *Proc. Natl. Acad. Sci. USA* **112**, E5237 (2015).
- [21] A. J. H. McGaughey and C. A. Ward, *J. Appl. Phys.* **93**, 3619 (2003).
- [22] J. A. Riback, L. Zhu, M. C. Ferrolino, M. Tolbert, D. M. Mitrea, D. W. Sanders, M.-T. Wei, R. W. Kriwacki, and C. P. Brangwynne, *Nature (London)* **581**, 209 (2020).
- [23] H. Falahati and E. Wieschaus, *Proc. Natl. Acad. Sci. USA* **114**, 1335 (2017).
- [24] J. Lawrimore, D. Kolbin, J. Stanton, M. Khan, S. C. de Larminat, C. Lawrimore, E. Yeh, and K. Bloom, *Nucleic Acids Res.* **49**, 4586 (2021).
- [25] H. J. Wiedner and J. Giudice, *Nat. Struct. Mol. Biol.* **28**, 465 (2021).
- [26] I. Eshghi, J. A. Eaton, and A. Zidovska, *Phys. Rev. Lett.* **126**, 228101 (2021).
- [27] S. Talwar, A. Kumar, M. Rao, G. I. Menon, and G. V. Shivashankar, *Biophys. J.* **104**, 553 (2013).
- [28] A. Mahajan, W. Yan, A. Zidovska, D. Saintillan, and M. J. Shelley, *Phys. Rev. X* **12**, 041033 (2022).
- [29] C. M. Caragine, S. C. Haley, and A. Zidovska, *Phys. Rev. Lett.* **121**, 148101 (2018).
- [30] C. Cubeñas-Potts and V. G. Corces, *Nucleus* **6**, 430 (2015).
- [31] S. Boulon, B. J. Westman, S. Hutten, F.-M. Boisvert, and A. I. Lamond, *Mol. Cell* **40**, 216 (2010).
- [32] A. D. Stephens, E. J. Banigan, S. A. Adam, R. D. Goldman, and J. F. Marko, *Mol. Biol. Cell* **28**, 1984 (2017).
- [33] A. D. Stephens, E. J. Banigan, and J. F. Marko, *Curr. Opin. Cell Biol.* **58**, 76 (2019).
- [34] Y. Qi and B. Zhang, *Nat. Commun.* **12**, 6824 (2021).
- [35] C. M. Caragine, S. C. Haley, and A. Zidovska, *eLife* **8**, e47533 (2019).
- [36] D. Qian, T. J. Welsh, N. A. Erkamp, S. Qamar, J. Nixon-Abell, G. Krainer, P. S. George-Hyslop, T. C. T. Michaels, and T. P. J. Knowles, *Phys. Rev. X* **12**, 041038 (2022).
- [37] P. A. Chong and J. D. Forman-Kay, *Curr. Opin. Struct. Biol.* **41**, 180 (2016).
- [38] Y. Shin and C. P. Brangwynne, *Science* **357**, eaaf4382 (2017).
- [39] C. P. Brangwynne, C. R. Eckmann, D. S. Courson, A. Rybarska, C. Hoegel, J. Gharakhani, F. Jülicher, and A. A. Hyman, *Science* **324**, 1729 (2009).
- [40] D. M. Mitrea and R. W. Kriwacki, *Cell Commun. Signal.* **14**, 1 (2016).
- [41] N. M. Kanaan, C. Hamel, T. Grabinski, and B. Combs, *Nat. Commun.* **11**, 2809 (2020).
- [42] M. M. C. Tortora, L. D. Brennan, G. Karpen, and D. Jost, *Proc. Natl. Acad. Sci. USA* **120**, e2211855120 (2023).
- [43] C. Hult, D. Adalsteinsson, P. A. Vasquez, J. Lawrimore, M. Bennett, A. York, D. Cook, E. Yeh, M. G. Forest, and K. Bloom, *Nucleic Acids Res.* **45**, 11159 (2017).
- [44] C. J. Lawrimore, J. Lawrimore, Y. He, S. Chavez, and K. Bloom, *Mutat. Res.-Fund. Mol. M.* **821**, 111706 (2020).
- [45] C. Hanauer, S. Bergeler, E. Frey, and C. P. Broedersz, *Phys. Rev. Lett.* **127**, 138101 (2021).
- [46] S. M. Pachong, I. Chubak, K. Kremer, and J. Smrek, *J. Chem. Phys.* **153**, 064903 (2020).
- [47] K. Liu, A. E. Patteson, E. J. Banigan, and J. M. Schwarz, *Phys. Rev. Lett.* **126**, 158101 (2021).
- [48] K. Huang, Y. Li, A. R. Shim, R. K. A. Virk, V. Agrawal, A. Eshein, R. J. Nap, L. M. Almassalha, V. Backman, and I. Zsleifer, *Sci. Adv.* **6**, eaay4055 (2020).
- [49] D. S. W. Lee, N. S. Wingreen, and C. P. Brangwynne, *Biophys. J.* **120**, 318a (2021).
- [50] Y. Gao, X. Li, P. Li, and Y. Lin, *Nat. Chem. Biol.* **18**, 1307 (2022).

- [51] G. Schuette, X. Ding, and B. Zhang, *Biophys. J.* **122**, 3425 (2023).
- [52] S. Dillinger, T. Straub, and A. Nemeth, *PLoS ONE* **12**, e0178821 (2017).
- [53] Y. He, D. Adalsteinsson, B. Walker, J. Lawrimore, M. G. Forest, and K. Bloom, *Methods Mol. Biol.* **2415**, 211 (2022).
- [54] R.-H. Pusarla and P. Bhargava, *FEBS J.* **272**, 5149 (2005).
- [55] X.-Z. Cao and M. G. Forest, *J. Phys. Chem. B* **123**, 974 (2019).
- [56] See Supplemental Material at <http://link.aps.org/supplemental/10.1103/PhysRevE.109.L042401> for polymer chain model of chromatins; nonbonded pair interaction; dynamics equation of beads; LJ units; and binding and unbinding kinetics of crosslinks, which includes Refs. [63,64].
- [57] Y. Zhang, D. S. W. Lee, Y. Meir, C. P. Brangwynne, and N. S. Wingreen, *Phys. Rev. Lett.* **126**, 258102 (2021).
- [58] W. Thomson, *Proc. R. Soc. Edinb.* **7**, 63 (1872).
- [59] S. Izrailev, S. Stepaniants, B. Israilewitz, D. Kosztin, H. Lu, F. Molnar, W. Wriggers, and K. Schulten, *Ideas* (Springer-Verlag, Berlin, 1998), Vol. 4, pp. 39–65.
- [60] S. Park and K. Schulten, *J. Chem. Phys.* **120**, 5946 (2004).
- [61] C. Jarzynski, *Phys. Rev. Lett.* **78**, 2690 (1997).
- [62] X.-Z. Cao, H. Merlitz, and M. G. Forest, *J. Phys. Chem. Lett.* **10**, 4968 (2019).
- [63] K. Kremer and G. S. Grest, *J. Chem. Phys.* **92**, 5057 (1990).
- [64] A. E. van Giessen and E. M. Blokhuis, *J. Chem. Phys.* **131**, 164705 (2009).